

EVAPORATION PERFORMANCE OF A PLATE-TYPE HEAT EXCHANGER EMBOSSED WITH PYRAMID-LIKE STRUCTURES

H. Matsushima, Senior Researcher

Mechanical Engineering Research Laboratory, Hitachi, Ltd., Tsuchiura, Japan

M. Uchida, Researcher

Mechanical Engineering Research Laboratory, Hitachi, Ltd., Tsuchiura, Japan

ABSTRACT

A new type of plate heat exchanger for water-refrigerant systems such as chillers has been developed. Plates embossed with pyramid-like structures are stacked up to form the heat exchanger. Three pyramid sizes, namely, similarly shaped patterns with heights of 1.0, 1.2 and 1.5 mm, were evaluated. Measured heat-transfer coefficients corresponding to the three plate sizes (convective vaporization) show a weak correlation with channel height, and they are about one and a half to two times higher than those of commercial herringbone-type plate heat exchangers. Moreover, measured heat-transfer coefficient for water convection was found to be lower for the smaller channel height; however, it was still higher than that of conventional plate heat exchangers. It was also found that the plate surface with the pyramid height of 1.0 mm makes the plate heat exchanger more compact and reduces the pressure drop on the water side by nearly half.

1. INTRODUCTION

Reducing the size of heat exchangers, thus minimizing the size of refrigeration systems, is very attractive because we can save space by making the installation area of such systems smaller. Plate heat exchangers have the advantage of compactness, so they are replacing conventional heat exchangers such as shell-and-tube types.

Refrigeration systems using alternative refrigerants have been actively studied worldwide as attention to protecting the earth's environment has increased over recent years. Natural refrigerants such as ammonia, propane or carbon dioxide are advantageous in that they do not cause an increase in the earth's surface temperature. For refrigeration cycles using a natural refrigerant, indirect vapor-compression systems with water/brine as a secondary refrigerant are the most promising. Efficiency of these systems depends on the performance of intermediate heat exchangers that transfer heat between the refrigerant channel (hereafter, referred to as the "refrigerant side") and the water channel (the "water side"). Plate heat exchangers have extremely high heat-transfer coefficient; therefore, they are advantageous in terms of their high efficiency in a total system.

Most plate heat exchangers nowadays use plates with a herringbone pattern. However, such herringbone-type plate heat exchangers used in refrigeration applications suffer some problems; namely, a large pressure drop on the water side and a lower heat-transfer coefficient on the refrigerant side than that on the water side. It is therefore difficult to further reduce the size of herringbone-type plate heat exchangers.

In response to the above-described problems, we have developed a plate heat exchanger with a new plate pattern; namely, the plates are embossed with pyramid-like structures. The performance of this new plate heat exchanger as an evaporator for a water-refrigerant system was experimentally evaluated. Consequently, this new type of exchanger was found to be

superior to conventional herringbone-type plate heat exchangers in terms of heat-transfer rate and water-side pressure drop.

2. PLATE SURFACE

The developed heat exchanger is constructed of stacked plates as shown in Fig. 1. The plates are made of thin stainless steel and impressed with small pyramid-like embossed patterns. Figures 1(b) and (c) show how the plates are stacked: the center of each impressed pyramid is directly below the edge of the pyramid above, which, in turn, is below the center of the one above. This arrangement of pyramid plates is termed “stacking with half-pitch position shift”.

A refrigerant flow channel is formed between plates I and II, and a water flow channel between plates II and III. In this structure, a surface with a convex pattern is formed at the bottom of each flow channel, and one with a concave pattern is formed at the top of the channel [see Fig.1(c)]. The top of the lower plate and the bottom of the upper plate are connected by brazing. These connection points produce high strength against refrigerant pressure.

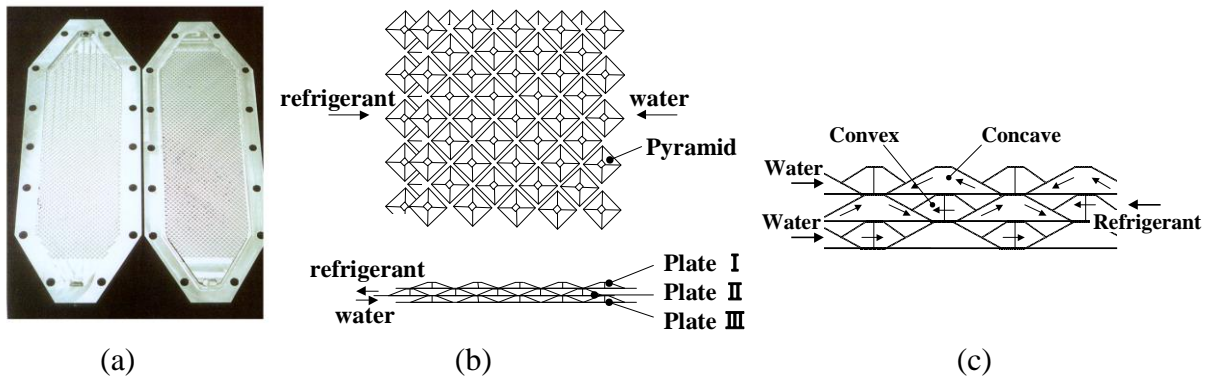


Fig. 1 Structure of plate surfaces with small pyramid-like embossed patterns

3. EXPERIMENTAL APPARATUS

A schematic of the experimental apparatus used in the study is shown in Fig. 2. A vapor-compression cycle was used to produce the refrigerant flow of which the evaporation heat-transfer coefficient was measured. For measuring the single-phase heat-transfer coefficient, water was circulated between the source water tank and the test section.

The test section models one channel of a plate heat exchanger. Passing water and refrigerant alternately simulates the conditions of a multi-layer heat exchanger. The test section consists of two aluminum blocks. An “O” ring is installed between the upper and lower aluminum blocks in order to seal them. This sealing prevents the leakage of refrigerant up to pressures of 1.6 MPa. Embossed patterns are made directly by machining the surface of the aluminum blocks to reduce the thermal resistance so that the surface temperatures can be measured accurately. The specifications of the test section are as follows: length of channel, 380 mm; width of channel, 100 mm; length of embossed patterns, 310 mm along flow direction.

Three types of pyramid-like pattern, similar in shape but different in size, were tested. Their dimensions are listed in Table 1. Note that the heights of the pyramid-like patterns are the same as the channel heights.

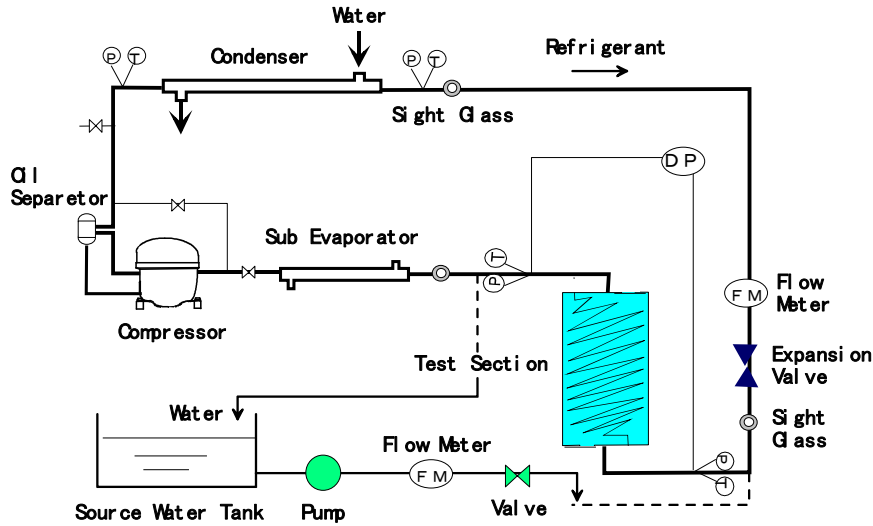


Fig. 2 Schematic of experimental apparatus

Table 1 Specifications of plate surfaces

Pattern type	Pyramid size (mm)	Pattern pitch (mm)	Plate size (mm)	Channel height (mm)
A	4.0 sq. × 1.5	5.0	380 × 100	1.5
B	3.2 sq. × 1.2	4.0	380 × 100	1.2
C	2.7 sq. × 1.0	3.37	380 × 100	1.0

For a rectangular flow channel with a low-aspect-ratio, the hydraulic diameter is almost double the channel height. Thus, it is 3.0 mm for type A, 2.4 mm for type B, and 2.0 mm for type C.

Two removable heater units are attached to the outer surfaces of the two aluminum blocks so they can be heated easily. In the heater unit, a sheath-type electric heater (length: 5.2 m; diameter: 1 mm) is bent into a zigzag and is directly soldered to the copper base plate. A thermal sheet is used to reduce the thermal resistance between the aluminum block and the heater unit. Thirteen T-type (copper-constantan) thermocouples with a diameter of 0.2 mm were implanted near the inner surface of each aluminum block in order to measure the local wall temperatures.

A turbine-type flow meter with a maximum flow rate of 40 l/min was used to measure the refrigerant flow. Refrigerant pressure and pressure drop were determined by a pressure transducer (maximum pressure: 2.1 MPa) and a differential pressure gauge (maximum pressure difference: 0.1 MPa); water flow rate was measured by a positive-displacement meter, and water-pressure drop was measured by a differential pressure gauge (maximum pressure difference: 500 kPa). Refrigerant R22, still the most popular refrigerant for chiller units, was used in the experiments. The flow rates of refrigerant and water, and the refrigerant-side pressures were set at values that would simulate an actual heat exchanger used under standard operation conditions, for example, refrigerant outlet pressure of 0.51 MPa (i.e., equivalent saturation temperature: 0.71 °C).

Vapor qualities of the refrigerant at the inlet of the test section were about 0.1 in all experiments. And vapor qualities at the outlet of the test section were calculated from the measured heat-transfer rate: 0.26 for heat flux of 3 kW/m², 0.41 for 6 kW/m², 0.73 for 12 kW/m² at refrigerant flow rate of 22 kg/h.

The heat-transfer coefficients on the refrigerant side and water side are defined as

$$h_w = \frac{q}{T_{wall} - \bar{T}_w} \quad \dots(1)$$

and

$$h_r = \frac{q}{T_{wall} - \bar{T}_r} \quad , \quad \dots(2)$$

where q is heat flux, T_{wall} is average wall temperature at the middle of the flow channel, \bar{T}_w is average water temperature between the inlet and the outlet of the flow channel, and \bar{T}_r is average refrigerant temperature between the inlet and the outlet of the flow channel (arithmetic mean values).

Heat flux q was determined from the electrical input to the heater and the surface area of each block in the channel. The surface area of each side of the test section (calculated by using projection area instead of total surface area) was 0.0328 m^2 .

4. EXPERIMENTAL RESULTS

4.1 Heat Transfer and Pressure Drop on the Water Side

Figure 3 plots water-side heat-transfer coefficients against the water flow rate measured in the experiments using the three plate surfaces (Table 1). Measured coefficients for the surfaces with a convex pattern and those with a concave pattern are indicated separately. Figure 4 plots the measured water-side pressure drop against the water flow rate for the three plate surfaces.

Data for plates with a herringbone pattern from other researchers and product catalogs are also plotted in Figs. 3 and 4 for the purpose of comparison. The main specifications of the herringbone plates are listed in Table 2. SWEP B25 (size: $520 \times 120 \times 70 \text{ mm}$) is a plate heat exchanger used in some of the Hitachi's 15-kW-class chillers. The pressure-drop data for the surfaces with pyramid-like structures and for the SWEP B25 heat exchanger consist of the pressure drops in the channel and those at the inlet and outlet ports. On the other hand, pressure drop data reported by Yan and Lin (1999) and Focke et al. (1985) are purely those in the channel.

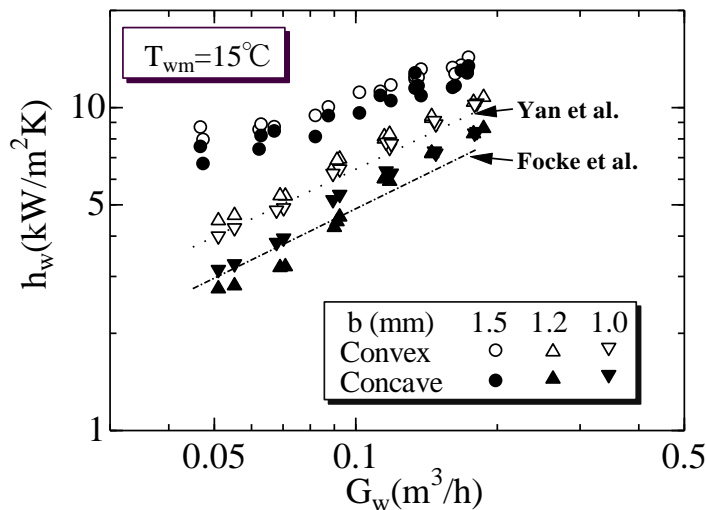


Fig. 3 Measured water-side heat transfer coefficient

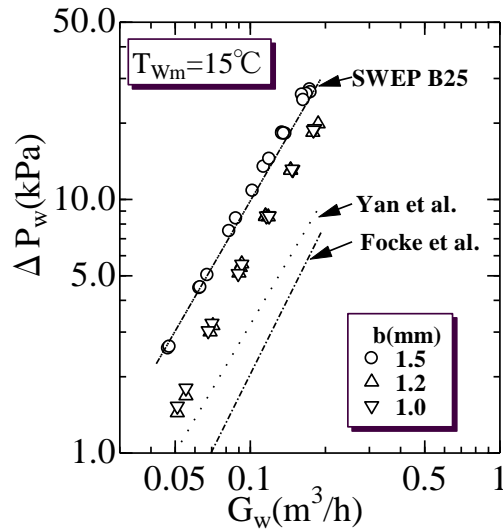


Fig. 4 Measured water-side pressure drop

Table 2 Specifications of herringbone plate surfaces

	Corrugation pitch (mm)	Plate size (mm)	Channel height (mm)
Yan et al. (1999)	10	500 × 120	3.3
Focke et al. (1985)	10	440 × 100	5.0
SWEP B25	about 7	520 × 120	about 2.0

The pressure drop at the inlet and outlet ports was empirically calculated according to Shah and Focke (1988). Using their correlation, we estimated the pressure drops at the inlet and outlet ports; that is, 7.1 kPa at a water flow rate of 0.2 m³/h and 1.7 kPa at 0.1 m³/h.

Figure 3 shows that plate type-A with a channel height of 1.5 mm has a single-phase heat-transfer coefficient of about 10 kW/m²K. This is an extremely high heat-transfer coefficient and similar to the highest value for herringbone-type plate heat exchangers (which can be found in catalog data). Types B and C (channel heights of 1.2 and 1.0 mm) have a single-phase heat-transfer coefficients of about 4 to 10 kW/m²K at water flow rates of 0.05 to 0.2 m³/h. These values are about half of type A's. However, they are still considered high enough for the plate surface of an evaporator. This is because the evaporation heat-transfer coefficient of a plate-type evaporator is usually lower than the water-side heat-transfer coefficient. A water-side heat-transfer coefficient over 10 kW/m²K is thus not required.

According to Fig. 4, the type-A plate with a channel height of 1.5 mm has the highest pressure drop among the three tested plate surfaces. The pressure drop in the channel of plate type A is almost the same as that of a conventional herringbone-type plate heat exchanger for a 15-kW chiller (SWEP B25). The pressure drops corresponding to types B and C are similar and nearly half of that corresponding to type A; their maximum values are about 20 kPa. Note that channel heights of types B and C are about 50 to 70% of that of the SWEP B25 plate.

As stated before, heat-transfer coefficient and pressure drop corresponding to types B and C are about half of those corresponding to type A. However, heat-transfer coefficients for all three plate surfaces are considered high enough. Regarding the use of the present surfaces as an evaporator, the lower-pressure-drop characteristics of types B and C are preferable. Furthermore, their smaller channel heights enable fabrication of a high-performance, very

compact plate heat exchanger.

Incidentally, there is only a little difference between the heat-transfer coefficient and pressure drop of types B and C. Because the effective Reynolds number is decreased by reducing channel height, we expect three-dimensional turbulence in the channel to be reduced and that flow patterns will be very similar under curtain Reynolds numbers.

4.2 Heat Transfer and Pressure Drop on the Refrigerant Side

When plate-type exchangers are used as evaporators, they are usually used in a counter-flow setup with the flow direction vertical to the ground. Thus, the water side is the “down flow” side and the refrigerant side is the “up flow” side. This kind of setup is particularly effective for a refrigeration cycle using a zeotropic refrigerant mixture such as R407C.

Figures 5 through 8 show evaporation heat-transfer coefficients and pressure drops for plate surfaces in the above-mentioned flow-direction setup. Here, refrigerant flow rate and pressure drop can be converted into other parameters for reference. Thus, refrigerant flow rate of 10 kg/h corresponds to a mass velocity of 18.5 kg/m²s for type A, 23.1 kg/m²s for type B and 27.8 kg/m²s for type C when channel width is 100 mm. The refrigerant-side pressure drop of 10 kPa is equivalent to a pressure drop per unit length of 26 kPa/m when channel length is 380 mm.

Figure 5 plots experimental evaporation heat-transfer coefficient against refrigerant flow rate at heat flux of 12 kW/m². Data for plates with a herringbone pattern from other researchers are also shown for the purpose of comparison. Namely, Yan and Lin (1999) reported an experiment on evaporation using refrigerant R134a under similar conditions of mass velocity and average vapor quality. The main specifications of their herringbone plates are listed in Table 2. Moreover, Thonon, et al. (1995) proposed an empirical correlation for estimating evaporation heat-transfer coefficient in herringbone plates, and data calculated from their correlation is plotted in Fig. 5.

Figure 5 shows that the evaporation heat-transfer coefficient estimated from Thonon’s correlation is between 2 and 3 kW/m²K. This is almost the same as the heat-transfer coefficient of convective vaporization measured in bare tubes (Webb 1994). Pelletier and Palm (1997) also reported that the evaporation heat-transfer coefficient of a herringbone-type plate heat exchanger is below 2 kW/m²K at a heat flux up to 10 kW/m² (refrigerant R22). They showed this heat-transfer coefficient is close to that of nucleate pool boiling. Therefore, a phenomenon similar to the nucleate boiling of smooth surfaces might occur at the surface of herringbone plates.

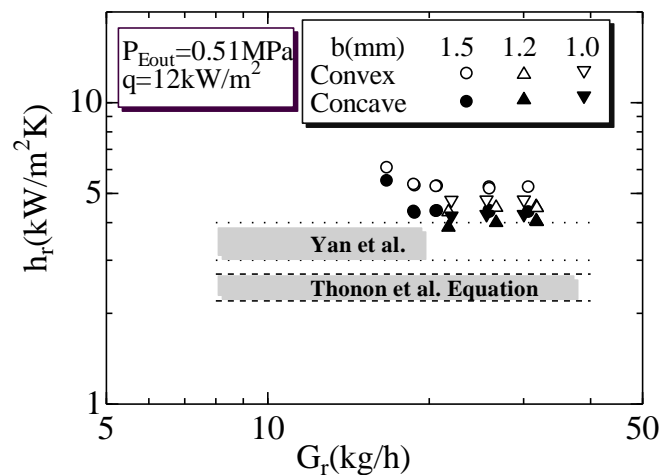


Fig. 5 Measured evaporation heat-transfer coefficients of vertically set plates

It is also clear from Fig. 5 that the evaporation heat-transfer coefficients of all the plates are almost the same. Although the heat-transfer coefficients of the surfaces with convex patterns are slightly higher than those of the surfaces with concave patterns, there is no significant difference. It is also shown that the evaporation heat-transfer coefficients of the tested plate surfaces are 1.5 to 2 times higher than those of currently used herringbone-type plates.

Figure 6 shows that the pressure drops along the refrigerant channel are less than 16 kPa within the range of experimental conditions. This is almost the same value as that reported by Yan and Lin (1999) under the same conditions. The difference in the pressure drops corresponding to the three channel heights is relatively small.

The measured pressure drops corresponding to the three plates include those at the inlet and outlet ports; those reported by Yan and Lin (1999) do not. The estimated pressure drop at the inlet and outlet ports calculated by the correlation proposed by Shah and Focke (1988) is roughly 2 to 3 kPa at a refrigerant flow rate of 20 kg/h and 4 to 7 kPa at 30 kg/h.

A close look at the effect of the channel height on the evaporation performance shows (Figs. 5 and 6) that the heat-transfer coefficient corresponding to type C is slightly higher than that corresponding to type B. It is also clear that pressure drop corresponding to type C is slightly lower than that corresponding to type B. These characteristics are preferable from the viewpoint of performance and compactness of plate heat exchangers. The reason for the slight increase in heat-transfer coefficient corresponding to type C might be that the number of nucleus points is higher when the dimensions of the embossed pattern are smaller. The reason for the slight decrease in pressure drop corresponding to type C is due to reduction of the effective Reynolds number and three-dimensional turbulence in the channel.

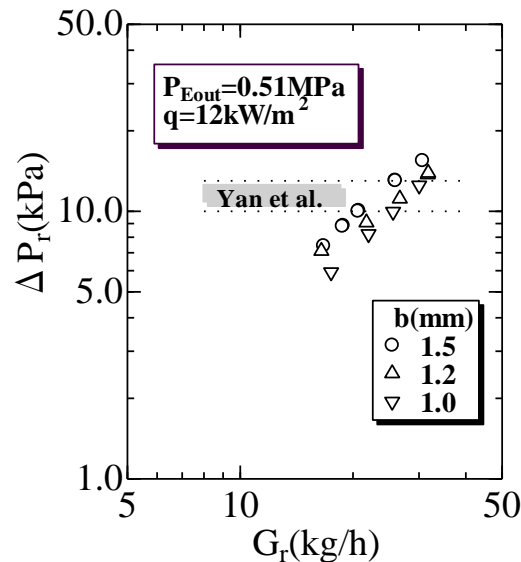


Fig. 6 Measured refrigerant-side pressure drop of vertically set plates

Figures 7 (heat flux : 3 kW/m²) and 8 (heat flux : 12 kW/m²) show variation of evaporation heat-transfer coefficients of all surfaces along the flow direction when the plates are set vertically. On the x-axis, Z is the distance measured from the inlet to the measurement point (pyramid-like embossed patterns are formed between Z of 0.035 and 0.345 m).

Figure 7 shows that the evaporation heat-transfer coefficient of the surface with convex patterns and a 1.5-mm channel height (type A) increases rapidly in the flow direction. In contrast, the increase in heat-transfer coefficient corresponding to the other channel heights (types B and C) of the convex pattern is not so steep. Figure 7 also shows the variation of heat-transfer coefficient along the flow direction of the surfaces with concave patterns is not so large compared to that in the case of the convex surface. There are three possible reasons for these tendencies. First, the wetness of the convex surface is so high that a layer of thin liquid film usually stays on the surface. Second, the turbulence increases because of the increase in refrigerant velocity, especially when channel height is larger. These two reasons explain the higher heat-transfer coefficient on the convex-surface side. Third, regarding the concave-surface side, a “re-circulation” pattern is formed in the vicinity of the concave surface. Therefore, the heat-transfer coefficient there has a weak correlation with the increase in refrigerant velocity.

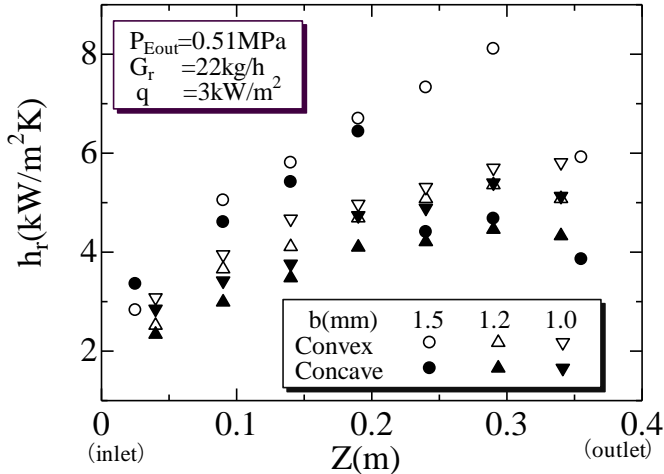


Fig. 7 Variation of evaporation heat-transfer coefficient along the flow direction on vertically set plates (heat flux of 3 kW/m²)

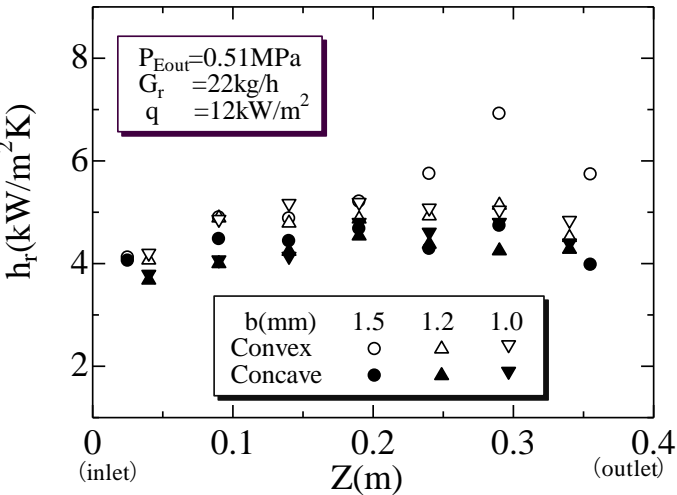


Fig. 8 Variation of evaporation heat-transfer coefficient along the flow direction on vertically set plates (heat flux of 12 kW/m²)

This difference between the heat-transfer coefficients of the convex surfaces and concave

surfaces disappears at heat flux of 12 kW/m² (Fig. 8). This is because the flow in the channel becomes nearly homogeneous as a result of an increasing number of bubbles with increasing heat flux. Therefore, there is a high possibility that local dry-out spots will occur on both surfaces. Yan and Lin (1998), who used refrigerant R134a, also reported a decrease in evaporation heat-transfer coefficient in a small pipe (diameter of 2 mm) at high vapor quality when heat flux is increased. They considered that the occurrence of local dry-out spots on the tube wall may cause this decrease.

Incidentally, regardless of heat flux, heat-transfer coefficients along the flow direction of the convex and concave surfaces with channel heights of 1.2 and 1.0 mm (types B and C) are similar and remain relatively lower than that of a convex surface with a 1.5-mm channel height (type A). This result also might be a result of a similar phenomenon to local dry-out spots that occurs in a small pipe, because the hydraulic diameters corresponding to types B and C are rather small, 2.4 and 2.0 mm, respectively.

5. EVALUATION OF THREE PYRAMID-EMBOSSSED SURFACES AS EVAPORATORS

We evaluated the heat-transfer performance of a plate-type evaporator with three different pyramid-like patterns. In this evaluation, we first assumed that the plate heat exchanger is constructed by stacking the pyramid plate in a multi-layer structure, and passing water and refrigerant in the channels between the layers alternately. Plate size was assumed to be identical to that of the three tested surfaces, and the only difference between assumed and tested surfaces is the structure of the inlet and outlet ports, which is modified to be the same as that of conventional plate heat exchangers. We also assumed that cooling capacity is 15 kW and that type A has 13 channels and types B and C have 14.

Under these assumptions, the present heat exchanger would have a height of 0.36 m, a depth of 0.058 m, and a width of 0.106 m for type A; a height of 0.36 m, a depth of 0.054 m, and a width of 0.106 m for type B; a height of 0.36 m, a depth of 0.048 m, and a width of 0.106 m for type C. These dimensions are approximately 50%, 52% and 58% less volume than that of conventional herringbone-type plate heat exchangers with the same cooling capacity (SWEP: B25, 0.52 × 0.07 × 0.12 m).

We estimated the heat-transfer performance of heat exchangers with the above-mentioned dimensions. Heat-transfer rate of a heat exchanger, Q , is expressed as

$$Q = \varepsilon (\dot{m}C_p)_{\min} (T_{w_{in}} - T_{r_{in}}) \quad , \quad \cdots(3)$$

where ε is heat exchanger effectiveness, $(\dot{m}C_p)_{\min}$ is minimum heat capacity rate for fluids, and $T_{w_{in}}$ and $T_{r_{in}}$ are inlet temperatures of water and refrigerant, respectively. Refrigerant temperature is almost constant within the channel during the course of evaporation. Therefore, effective heat capacity rate of the refrigerant is extremely large; accordingly, heat capacity rate of the water is smaller, so it is used as a minimum value.

The heat exchanger effectiveness ε has the following relation with number of heat transfer units (NTU) and other parameters when a phase change occurs in the fluid:

$$\varepsilon = 1 - \exp(-NTU) \quad \cdots(4)$$

$$NTU = \frac{UA}{(\dot{m}C_p)_{\min}} \quad \cdots(5)$$

$$1/U = 1/h_w + 1/h_r, \dots(6)$$

where U is overall heat-transfer coefficient and A is heat-transfer area of each flow channel. In Eq. (6), conduction thermal resistance in the tube wall is neglected because it is small enough compared with convection thermal resistance. Estimated overall heat-transfer coefficients of the three plate surfaces are given in Table 3. As the flow-area size of the embossed plate is about 0.1×0.31 m, A is 0.062 m^2 . Although water flow rate under standard operating conditions of chillers with 15-kW cooling capacity is $2.5 \text{ m}^3/\text{h}$, water flow rate per channel is $0.192 \text{ m}^3/\text{h}$ for type A and $0.18 \text{ m}^3/\text{h}$ for types B and C. Substitution of these values into Eq. (4) gives the effectiveness of the plate surfaces as 0.600 for type A, 0.565 for type B, and 0.579 for type C.

Table 3 Heat-transfer coefficients of plate surfaces

TYPE	Channel height (mm)	Evaporation heat transfer coefficient h_r (kW/m ² K)	Water side heat transfer coefficient h_w (kW/m ² K)	Flow rate of Water (m ³ /h)	Overall heat transfer coefficient U (kW/m ² K)
A	1.5	5.00	10	0.06 to 0.18	3.3
B	1.2	4.00	4.0	0.06	2.0
			7.5	0.12	2.6
			9.5	0.18	2.8
C	1.0	4.25	4.0	0.06	2.1
			7.0	0.12	2.6
			9.3	0.18	2.9

We estimated the heat-transfer rate of a heat exchanger by using Eq. (3). In this calculation, we set water inlet temperature to 12°C and refrigerant inlet temperature to 1.6°C (referring to actual operating conditions of evaporators for chillers). We assumed a saturated condition with inlet pressure of 0.525 MPa in order to estimate the refrigerant inlet temperature. (It is clear from Fig. 6 that pressure drop is nearly 15 kPa when outlet pressure is 0.51 MPa.) The estimated heat-transfer rates for each flow channel are 1.39 kW for type A, 1.19 kW for type B, and 1.27 kW for type C. Therefore, total heat-transfer rates for all channels are 18.1 kW for type A, 16.6 kW for type B, and 17.7 kW for type C. These values are respectively 20%, 11%, and 18% higher than the target heat transfer rate of 15 kW.

Pressure drop in the water channel for the above cases was evaluated. According to Fig. 4, the measured water-side pressure drops are about 33 kPa for type A, 20 kPa for type B, and 19 kPa for type C. The pressure drop corresponding to type A (33 kPa) is almost the same as that in a currently used herringbone-type plate heat exchanger with the same cooling capacity (SWEP: B25; $0.52 \times 0.07 \times 0.12$ m). Moreover, pressure drops corresponding to types B and C are approximately 40% less than those in a herringbone-type plate heat exchanger.

Using the estimation procedure outlined above, we determined appropriate specifications for a heat exchanger that would reduce the pressure drop on the water side by 50% compared to that with a currently used herringbone-type plate heat exchanger. We set the target value of the water-side pressure drop as 16.5 kPa at a total water flow rate of $2.5 \text{ m}^3/\text{h}$. In the following, plate type C is used as an example because it has the best heat-transfer performance and is the most compact.

First, the water flow rate that produces a pressure drop of 16.5 kPa was determined. (Figure 4 gives per channel water flow rate for this case as $0.168 \text{ m}^3/\text{h}$.) According to the total water-flow rate stated above, the number of flow channels should be 15. The specification of

the heat exchanger is thus given as a height of 0.36 m, a depth of 0.051 m, and a width of 0.106 m. This is approximately 45% of the size of currently used herringbone-type plate heat exchangers with 15-kW cooling capacity (SWEP: B 25).

We chose the overall heat-transfer coefficient as $2.9 \text{ kW/m}^2\text{K}$ from Table 3. Substitution of this value and heat capacity rate at a water-flow rate of $0.168 \text{ m}^3/\text{h}$ into Eqs. (4) and (5) gives a heat-exchanger effectiveness of 0.602. When the inlet temperatures of water and refrigerant are set to 12°C and 1.6°C , the heat-transfer rate for each channel is obtained from Eq. (3) as 1.26 kW. Therefore, total heat-transfer rate for 15 channels is 18.9 kW, which is sufficiently higher than the target heat transfer rate of 15 kW.

Table 4 Estimated pressure drops and volume ratios in evaporators using three pyramid plates

Case No.	Specification (Cooling capacity of 15 kW)	Pressure drop on water side at standard flow rate of $2.5 \text{ m}^3/\text{h}$	Volume ratio
1	Type A (b = 1.5 mm) Size: $0.36 \times 0.106 \times 0.058 \text{ m}^3$ Number of channels: 13	33 kPa	0.50
2	Type B (b = 1.2 mm) Size: $0.36 \times 0.106 \times 0.054 \text{ m}^3$ Number of channels: 14	20 kPa	0.48
3	Type C (b = 1.0 mm) Size: $0.36 \times 0.106 \times 0.048 \text{ m}^3$ Number of channels: 14	19 kPa	0.42
4	Type C (b = 1.0 mm) Size: $0.36 \times 0.106 \times 0.051 \text{ m}^3$ Number of channels: 15	16.5 kPa	0.45
Reference	Herringbone plate (SWEP:B25) Size: $0.52 \times 0.12 \times 0.07 \text{ m}^3$ Number of channels: 13	33 kPa	1.0

The estimated pressure drops and volume ratios are summarized in Table 4. From the viewpoint of compactness, lower channel height in the case of types B and C is clearly superior to the higher overall heat-transfer coefficient (Table 3) in the case of type A. Moreover, plate type C (cases 3 and 4) with a channel height of 1.0 mm is superior to the others in terms of compactness. In particular in case 4, both volume ratio and water-side pressure drop are reduced by about 50% compared to a conventional herringbone-type plate heat exchanger with the same cooling capacity.

6. SUMMARY

The evaporation performance of a new plate heat exchanger for water-refrigerant systems such as chillers was investigated experimentally. In this heat exchanger, many small embossed-patterns with a pyramid-like structure are formed on the plate surface. To investigate the dependence of embossed pattern size on heat-transfer performance, three pyramid sizes, namely channel heights of the similarly shaped embossed patterns of 1.0, 1.2, and 1.5 mm, were studied. The results of the study are summarized as follows.

- Measured evaporation heat-transfer coefficients on the tested plates are about 1.5 to 2 times higher than those of commercially used herringbone-type plate heat exchangers, and they have a weak correlation with channel height.

● Measured single-phase heat-transfer coefficient corresponding to the plate with a channel height of 1.5 mm is comparable to the highest value for herringbone-type plate heat exchangers. Measured single-phase heat-transfer coefficients corresponding to plates with channel heights of 1.2 and 1.0 mm are about half that value; however, they are still high enough for evaporators.

● Measured pressure drop corresponding to the plate with a channel height of 1.5 mm is the highest of the three tested plate surfaces. This value is almost the same as the pressure drop of conventional herringbone-type plate heat exchangers for 15-kW class chillers. Measured pressure drops corresponding to plates with channel heights of 1.0 and 1.2 mm are almost the same and are nearly half those corresponding to the plate with 1.5-mm channel height.

● From the viewpoint of compactness, the plates with channel heights of 1.2 and 1.0 mm are better than 1.5-mm-channel-height plate, in spite of their lower overall heat-transfer coefficient. Of these two, the plate with a 1.0-mm channel height is the best in terms of compactness. It is thus concluded that, compared to a conventional herringbone-type plate heat exchanger with the same cooling capacity, we can make a plate heat exchanger more compact and reduce the pressure drop on the water side by nearly half, by using the 1.0-mm-channel-height plate.

REFERENCES

Focke, W. W., et al. 1985. The Effect of the Corrugation Inclination Angle on the Thermohydraulic Performance of Plate Heat Exchangers, *Int. J. Heat Mass Transfer*, Vol. 28, pp. 1469-1479.

Pelletier, O. and Palm, B. 1997. Boiling of Hydrocarbons in Small Plate Heat Exchangers, *Proceedings of IIF-IIR, Commission B1, with E1 & E2*, pp. 231-241.

Shah, R. K. and Focke, W. W. 1988. Plate Heat Exchangers and Their Design Theory, in *Heat Transfer Equipment Design*, Eds. R. K. Shah et al., pp. 227-254, Hemisphere, Washington DC.

Thonon, B., et al. 1995. Recent Research and Developments in Plate Heat Exchangers, *J. of Enhanced Heat Transfer*, Vol. 2, Nos. 1-2, pp. 149-155.

Webb, R. L. 1994. *Principles of Enhanced Heat Transfer*, John Wiley & Sons, pp. 432-450.

Yan, Y. Y. and Lin, T. F. 1998. Evaporation Heat Transfer and Pressure Drop of Refrigerant R-134a in a Small Pipe, *Int. J. Heat and Mass Transfer*, Vol. 41, pp. 4183-4194.

Yan, Y. Y. and Lin, T. F. 1999. Evaporation Heat Transfer and Pressure Drop of Refrigerant R134a in a Plate Heat Exchanger, *Journal of Heat Transfer*, Vol. 121, pp. 118-127.